KES Transactions on Sustainable Design and Manufacturing I
Sustainable Design and Manufacturing 2014 : pp.720-731 : Paper sdm14-107

An experimental and CFD investigation into the mixing in a closed system stirred vessel

Jennifer Thompson[1], Diane McBride[1], Benjamin P. Wilson[1], Oubay Hassan[1], Sue Plummer[2], David Bould[1], Sam Rolland[1], Nick Lavery[1], Hans Sienz[1]

College of Engineering, Swansea University, Swansea, SA2 8PP, UK
jennifer.thompson@swansea.ac.uk[1]
Cultech Limited, Baglan Industrial Park, Port Talbot, SA12 7BZ, UK[2]

Abstract An investigation has been undertaken into the mixing mechanisms involved in a closed tank stirred vessel utilising a wide paddle agitator, for fluids in the viscosity range of 1 to 5.5 mPa s. In particular, the effect of fill depth on the mixing time has been considered, as this has a direct impact on the usability of the mixing process equipment for scaled-down batch production. Experimental work has been undertaken and this has been used to develop a suitable computational fluid dynamics (CFD) model which implements the Multiple Reference Frame (MRF) approach with the addition of a virtual tracer used to calculate mix time. A study into whether laminar or turbulent models are required and an appropriate method for the implementation of turbulence has been established. The results allow identification of the optimum ratio of fill depth to paddle height to be established. Additionally, the developed CFD model will allow for further investigation into the effects of other process parameters.

1. Introduction

The process of mixing is used in numerous industrial sectors including but not limited to, food, pharmaceutical and petrochemical. Small and medium sized companies or SMEs need to invest judiciously in mixing equipment that can be used flexibly through the range of products which they produce, of varying batch sizes and viscosities. On consultation with a local food supplement Production Company, a mixing process involving a closed system cylindrical vessel utilising a large paddle agitator has been identified, with a diameter of approximately 0.88 of the vessel width. The company employs this system for the manufacture of products over a range of viscosities and is required to scale up and down production quantities, especially for new products. Subsequently, an experimental and computational fluid dynamic (CFD) based investigation is to be undertaken for this stirred system, for fluids of viscosity range 1 to 5.5 mPa s. Typically, the quantification of a mixing system is defined in terms of the dimensionless Reynolds Impeller number Re_i, expressed in a stirred tank as a function of the fluid's density, ρ and dynamic viscosity, μ, the tank's diameter, D and the rotor speed, N in rev/s [1]:

$$Re_i = \frac{\rho N D^2}{\mu} \qquad \text{Equation 1}$$

However, this dimensionless term does not take into consideration the effect of fill level, with optimisation of this parameter critical to an efficient mixing process. Experimental work has been used to validate a CFD model and simulations performed to identify critical operational parameters that allow for optimisation of the process. Reducing mixing time and subsequent overhead costs, such as power and equipment wear. Improved understanding of the mixing mechanisms allow for potential scaling of the process for more economical and sustainable production.

2. Background

Three mechanisms can be identified in the stirred vessel mixing process: distribution, dispersion and diffusion. Distribution involves the bulk circulation of the fluid and is also termed *macromixing* [2]. Dispersion occurs at intermediate length-scales (larger than the Kolmogrov scale), hence is also termed *mesomixing* [2] and it is the result of turbulence within the stirred vessel. Mixing on a smaller scale is achieved via diffusion or *micromixing* [2, 3], a relatively slow process but efficient over small length scales. In stirred vessels the flow undergoes transition between laminar and turbulent regimes gradually, with the actual transition regime Re_i dependent upon factors including the system's geometry, impeller speed, viscosity of fluid, etc. The flow regime is deemed fully turbulent at Re_i > 10,000 [2, 3].

Mixing in liquids with low viscosities like water, with viscosity of 1 mPa s, tends to occur via momentum transfer and turbulence i.e. a combination of distribution and dispersion effects. High velocity streams produced by the rotation of the impeller entrain the slower moving, stagnant regions in all parts of the vessel, promoting a uniform mix. However, as the viscosity of the fluid is increased frictional drag forces retard the high velocity streams, confining them to the immediate vicinity of the impeller [4]. There are an extensive range of impeller types available for mixing, and the American Institute of Chemical Engineers [1] provides an excellent overview of the main designs available. A simple yet commonly used form of stirrer in industrial processes is the paddle. This type of impeller tends to operate at low rotational speeds and has a large blade area allowing it to push or carry liquid in a circular path around the vessel. The larger the surface area of the blade, the larger the volume of fluid moved. However, such a paddle produces no high velocity streams and subsequently there is very little top-to-bottom turnover within the mixing vessel. Moreover, operation of these types of paddles in low viscosity fluids will tend to produce a severe vortex effect i.e. similar to a whirlpool effect, even when operated at a moderate Re_i. So, their use is generally restricted to the mixing of highly viscous fluids, since they do not mix by a mechanism which requires the production of high velocity streams.

The parameter most convenient to use in the assessment of efficient mixing is mixing time. This can be assessed by the addition of a tracer into a vessel, which is deemed "mixed" when the concentration of tracer levels out to a constant value. Assuming initially there is no tracer present in the vessel, mixing time t_m can be defined as the time between the tracer addition to the time when:

$$\frac{|C - C_\infty|}{C_\infty} = m \qquad \text{Equation 2}$$

Where, C is the concentration of tracer, C_∞ is the tracer equilibrium value and m is the maximum acceptable deviation from homogenous conditions [5]. Usually, mixing time is defined as the amount of time elapsed until the tracer concentration differs from the final concentration by less than 10%, i.e. t_{90} the mixing time at which the tank is 90% mixed. Numerous techniques exist to experimentally determine mixing time, with the simplest comprising the visual assessment of a chemical tracer e.g. the (dye) decolourisation method. Dye decolourisation involves the inclusion of one chemical (or one chemical and an indicator) to the vessel to provide colour. Followed by the addition of another chemical – a tracer, which removes the colour from the vessel due to an effectively instantaneous chemical reaction. This method has the advantage of clearly highlighting any poorly mixed regions as pockets of colour. Generally however, mixing time based on the visual observation approach remains subjective [6] and can only be employed as an experimental technique when utilising a transparent bulk mixing fluid, in a transparent mixing vessel. Due to the limitations and difficulties involved when using experimental techniques to attain measurements of fluid properties within a mixing vessel, the CFD modelling of mixing in process industries has attracted attention since the early 1990s [7].

3. Governing equations of mixing simulations

Extensive work has been undertaken on the topic of rotational based mixing, in areas as diverse as helicopter rotor design [8] to stirred vessel chemical reactors [2]. Three main methods are available for simulation of mixing in a stirred vessel: the Virtual Blade Method (VBM); Multiple Reference Frame (MRF) Method; and the Sliding Mesh Method (SMM). These methods have been listed in order of increasing accuracy and subsequently increasing complexity and computational expense. In a recent review of work which utilised various modelling methods [5], it was concluded that on comparison, steady state methods like the MRF approach gave reasonably accurate approximations of flow field features, whilst saving around one-seventh on CPU time [9]. Based on a review of the literature, the MRF method is identified as the most commonly utilised approach for the assessment of mixing time in a stirred vessel with work undertaken by [7], [10], [11] [12], [13] and [2], all providing examples of the application of the MRF method.

The MRF method is a steady-state approach that involves the calculation of one flow field for a particular impeller or mixing blade position. It utilises a modified version of the Navier-Stokes equations. Where, Source terms are added to the momentum equation to account for centrifugal forces. For an incompressible fluid (i.e. such as the fluids to be modelled) the steady state governing equations comprise the continuity equation:

$$\nabla . \boldsymbol{u} = \boldsymbol{0} \qquad \text{Equation 3}$$

and the momentum equation:

$$\rho \nabla . (\boldsymbol{uu}) = -\nabla p + \nabla . [\mu \nabla \boldsymbol{u}] + S \qquad \text{Equation 4}$$

Where, $\boldsymbol{u}$ represents the velocity vector, p is pressure, μ is the dynamic viscosity and S comprises source terms added into Equation 4. Considering Figure 1 [14]: $\boldsymbol{v}$ is the absolute velocity as viewed from the stationary frame; the rotating reference frame has an angular velocity of $\boldsymbol{\omega}$; $\boldsymbol{v_r}$ is the relative velocity as viewed from the rotating frame at a position vector $\boldsymbol{r}$ from the origin of the rotating frame; and $\boldsymbol{u_r}$ is the whirl velocity due to the moving frame. Subsequently, fluid velocities are transformed from the stationary frame to the rotating frame using [5]:

$$\boldsymbol{v_r} = \boldsymbol{v} - \boldsymbol{u_r} \qquad \text{Equation 5}$$

Where, whirl velocity can be defined as:

$$\boldsymbol{u_r} = \boldsymbol{\omega} \times \boldsymbol{r} \qquad \text{Equation 6}$$

Defining a term known as the centripetal acceleration as:

$$S_{centripetal} = \boldsymbol{\omega} \times \boldsymbol{\omega} \times r \qquad \text{Equation 7}$$

And, a term known as the Coriolis acceleration as:

$$S_{Coriolis} = 2\boldsymbol{\omega} \times \boldsymbol{v_r} \qquad \text{Equation 8}$$

In the MRF approach the Coriolis and centripetal terms are added to the momentum equations as Source terms. Face interpolation techniques are required on the cell zone interfaces when solving using relative velocities (Figure 1). The velocity for any stationary surfaces must be specified as zero in the *inertial r*eference frame and transformed to relative velocities. When the absolute velocity formulation is used, Coriolis and centripetal effects can be collapsed as a single source term [5]:

$$S_{abs} = \boldsymbol{\omega} \times \boldsymbol{v} \qquad \text{Equation 9}$$

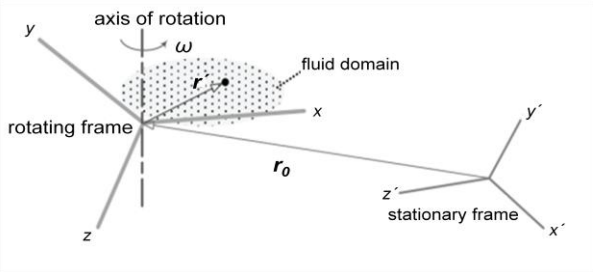

Figure 1 – Rotating frame position relative to Stationary frame position [14]

Generally in the simulation of stirred vessels, turbulence effects are modelled utilising the standard κ-ε model of Launder and Spaulding [15]. This turbulence model in conjunction with the MRF approach has been employed in work undertaken by [10], [11], [13] and [2]. A simpler algebraic model has also been applied to quantify turbulence effects, Croft *et al.*[16], here an effective viscosity value is obtained by multiplying the laminar velocity by an appropriate factor (A):

$$\mu = A * \mu_{lam} \quad \text{Equation 10}$$

Once a steady state flow field has been generated by the MRF method, a transient approach is employed for the prediction of mixing time. In simulation work undertaken by [5], after obtaining a converged steady state flow field a transient scalar transport equation is solved to mimic the tracer approach taken experimentally. The dynamic distribution obtained by solving the Reynolds-averaged time-dependent scalar transport equation is based upon the assumption that the tracer is distributed in the vessel by convection and diffusion [17]:

$$\frac{\partial \rho\varphi}{\partial t} + \nabla\rho\boldsymbol{U}\varphi = \nabla\left(\rho D_m \nabla\varphi - \frac{\mu_t}{\sigma_t}\nabla\varphi\right) \quad \text{Equation 11}$$

Where, φ is the tracer volumetric fraction, $\boldsymbol{U}$ is the mean velocity vector, ρ is the fluid density, D_m is the molecular diffusivity, μ_t is the turbulent viscosity and σ_t is the turbulent Schmidt number. Molecular diffusivity is not a critical value, since the contribution of molecular diffusion to the overall tracer dispersion is negligible [12]. This approach of calculating a steady state flow field and then injecting a tracer concentration over the frozen flow field and monitoring transiently, was also successfully undertaken in [7], [11], [13] and [2].

4. Experimental Modelling

In order to establish confidence in any results generated by a CFD model of the stirred vessel mixing process, experimental work was undertaken in order to establish the effects of fill level and viscosity on mixing time. The mixing process was scaled to ensure dynamic similarity with the production mixing process, by using the impeller diameter as a constant ratio. To enable a visualisation method approach a pH change using phenolphthalein as an indicator was implemented, i.e. change from alkaline to acidic environment results in a change from fuchsia-pink to colourless. Experiments were undertaken using a glass vessel (0.43m in height, 0.275m diameter), and a small paddle impeller, with a paddle tip clearance of 0.016m. Paddle speed was kept constant for the tests at the lowest speed setting option, ~27rpm for the electric mixer (Heidolph, Model RZR 2041). This allowed the decolourisation reaction to be easily observed by eye; mixing at higher speeds would introduce a greater degree of subjectivity into the mixing times measured. Test solutions comprising either doubly distilled water only or solutions of *d*-glucose (Merck, Germany) with viscosities (ranging between 1.33 and 5.49

mPa s) were used to determine the effect of viscosity on the mixing efficiency. Different aliquots of these solutions were added to the test tank to a fill depth of 25, 50, 75 or 100%. Re_i values of 26572, 20729, 15068 and 5671 were calculated for the following fluid viscosities 1 mPa s (0% glucose), 1.33 mPa s (10% glucose), 1.90 mPa s (20% glucose) and 5.49 mPa s (40% glucose), respectively. Considering the height of the paddle in relation to the depth of fluid at the four different fill levels, the depth of fluid to paddle height ratios were calculated as 0.62, 1.23, 1.85 and 2.47 for the increasing fill levels, respectively.

In order to facilitate the decolourisation technique, described previously, additions of both 1M potassium hydroxide (Merck, Germany) and phenolphthalein in ethanol solution (Sigma) were made in a ratio of 3ml to 1ml -per 25% of fill- to generate a fuchsia-pink colour characteristic of the phthalein indicator within the pH range 8.2 to 12.0. The time taken for the fuchsia-pink colour to disappear was recorded using a stop watch and video footage of the mixing was also captured. Figure 7 and Figure **2** show the effect of percentage fill on mixing time for the 1 mPa s solution, the effect of viscosity on mixing time at a 25% fill level and the effect of viscosity on mixing time at a 75% fill, respectively. Each mixing run was undertaken three times and the presented graphs show the subsequent averaged results ($\mp$ Standard Error (SE)). Larger SE values are observed for the lower fill levels at a viscosity of 1 mPa s (Figure 7), due to the inconsistency in the time taken for a trapped pocket of tracer to disperse. As the viscosity increases (Figure 2), the consistency in measured times also increases, resulting in lower SE values. Figure 3 provides an overview of images captured from video footage taken for the mixing process at 25% and 100% fills respectively. The trapped pockets of tracer are clearly evident at the 25% fill level

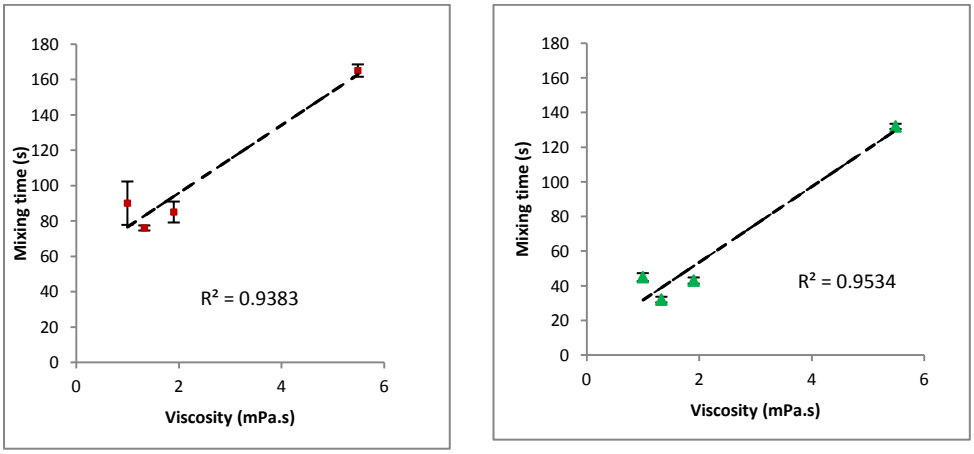

Figure 2 –Effect of viscosity on mixing time for (a) 25% and (b) 75% fill levels

Figure 3 - Time-lapsed photographic images throughout mixing of the decolourisation agent at (a) 25% and (b) 100% fill levels

5. Computational modelling

The commercial CFD software FLUENT 14.0 with the MRF technique implemented was employed for the simulation of a rotating paddle impeller at 27rpm in a fluid of viscosity 1 mPa s (i.e. water). Both laminar and turbulent simulations have been undertaken. For the turbulent simulations, the standard κ-ε turbulence model was implemented; however, due to unsatisfactory results generated from this approach a simpler algebraic model was adopted, for the implementation of turbulent effects.

Generally, the simulation process comprised three parts; part one involved the generation of geometry and hexahedral meshes using the software ICEM [18]. A mesh sensitivity analysis was carried out on the geometry for the 25% fill; it was found that a mesh size of 250,000 elements was required for independence. The same element size was then used to generate meshes for the deeper fill levels. Part two required the solution of the steady state flow field using FLUENT, the pressure-based solver with a relative velocity formulation was employed. Within FLUENT the “frame Motion” was set with a rotational velocity of 27rpm and the following boundary conditions set: the blade as a stationary wall; the vessel as a moving wall with zero absolute rotational velocity, the no-slip shear condition was applied; the surface of the fluid was set as a symmetry boundary condition. Initially, laminar flow fields were solved for the four different fill levels; in separate simulations, turbulent flow fields were solved using both the standard κ-ε turbulence model and the alternative approach of increasing the laminar viscosity by a factor of ten to simulate the viscosity effects of eddies. Part three of the simulation involved the addition of solving a scalar transport equation to represent a tracer on the generated flow fields (both laminar and turbulent for all fill levels). The flow field solution was frozen, then a scalar was introduced via an annulus inlet previously defined in the geometry construction (part 1); a set mass flow rate

was introduced, as used experimentally for the various fill levels, over 3 s with a 0.01 s time step. The inlet boundary condition was then set back to symmetry and the simulation solved transiently to determine how the scalar-tracer dispersed through the steady state flow field contours. The extent of mix was ascertained from the run model by using the ANSYS CFD post analysis tool. At various points in the vessel (virtual) probe locations were inserted (Figure 4 a), throughout the height and width of the mixing fluid. The scalar concentration versus time data was then extracted from each of these locations and analysed, with the probes placed at comparable positions for the different fill levels. When a constant scalar value (to 3.s.f) was attained (Figure 4 b), for all probes, the scalar contours were generated to check for the formation of any unmixed pockets away from the probe locations. If none were found then the time taken for 100% mixing to occur was established. If pockets of unmixed tracer were found then probes were placed at these specific locations and monitored until they also reached the constant concentration value.

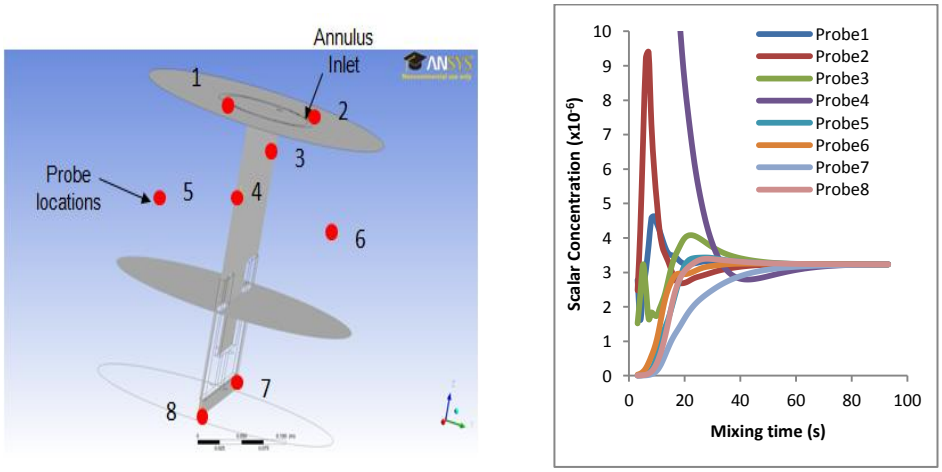

Figure 4 - Scalar concentration was measured at (a) probe locations throughout the mixing vessel the variation of scalar concentration with time could be plotted (b) an example of this for the 25% filled vessel

6. Results and discussion

On reviewing the experimental results a pattern of mixing occurred where: the higher the viscosity the longer the time taken to fully mix, explained by the increase in frictional drag forces retarding the generation of any high velocity streams and increasing time taken for flow to circulate and mix; and, perhaps counter-intuitively, the lower the percentage fill the longer the time taken to fully mix, caused by pockets of color becoming trapped (Figure 3 (a)). At deeper fill levels the fluid can

circulate more effectively around the height of the tank, thus promoting more efficient mixing via both distribution and dispersion effects. For the laminar simulations it became evident that the lower percentage fills were producing results that gave good comparison with the experimental data; whilst, the deeper fill levels were greatly over predicting the mix times measured. This could be explained by considering that the main mixing mechanism for the lower percentage fills would be due to the pushing effect of the paddle, there could be no movement of the fluid over and around the impeller. Subsequently, the laminar model is sufficient to capture this distributive only behaviour, despite the Re_i being calculated as turbulent. In contrast, the laminar solver becomes insufficient for the deeper fill levels as turbulence and hence dispersion effects will begin to contribute to the mixing mechanisms. The results from the initially implemented standard κ-ε turbulence model were found to generate non-physical flow fields (see **Error! Reference source not found.** b). The flow pattern indicated that the turbulence model raised turbulent viscosity to an extent which dampened any circulation of the fluid up and around the tank, producing a flow field that rotated just as one body. It is proposed that the inability of the model to simulate reality could be attributable to the lack of inlet/outlet boundary conditions in the model. Subsequently, appropriate turbulence intensity values could not be set, which resulted in any error that the model produced in estimating turbulence effects being trapped and magnified within the rotating fluid body. The work previously cited as using this turbulence model was not simulating such a simple closed system e.g. there was recirculation incorporated, which would overcome this issue [11].

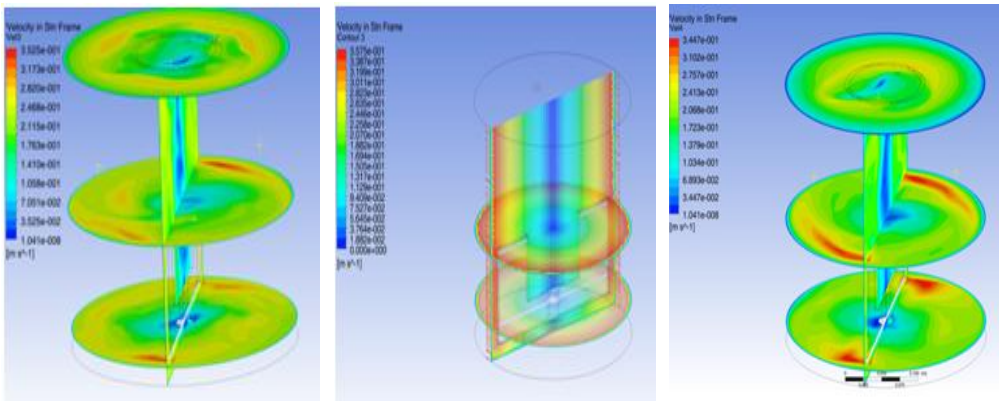

Figure 5 – Velocity contours for 100% fills using: a.) Laminar; b.) standard κ-ε and c.) linear algebraic (laminar) turbulent model

The results for the turbulent simulation using an algebraic turbulent viscosity value for the deep fills (75% and 100%) were found to generate more realistic flow fields

(Figure 5 (c)). The scalar-tracer distribution (Figure 6) and subsequently mixing times were more comparable to those viewed experimentally.

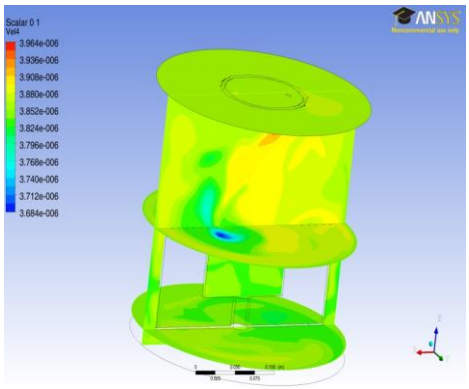

Figure 6 – Contours generated for tracer in 100% fill after 30s

Figure 7 provides an overview of the mixing times generated by the CFD simulations, using a laminar solver for the 25% and 50% fill levels and the algebraic turbulent viscosity model for the deeper fills, which compare favourably with the experimental work. R^2 values for both experimental and simulation results support that linear scaling of the mix time with fill level is appropriate. Therefore, the ratio of the depth of fluid to the paddle height for the closed vessel mixing system under consideration has a critical effect on the mixing time. Subsequently, the company must consider this when attempting to scale down batch production of a low viscosity fluid using their current setup.

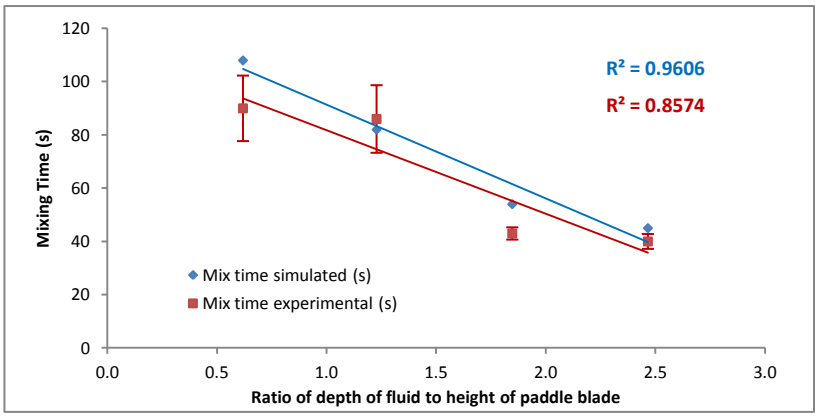

Figure 7 – The effect of vessel fill level on mixing time at viscosity of 1 mPa s – experimental and CFD results

7. Conclusions

From the small scale experimental and CFD simulation work, the mechanisms of mixing involved in fluid of viscosity in the range (1.0 to 5.5 mPa s) mixed by a paddle impeller have been investigated. A validated CFD model has been attained, which highlights the need to introduce turbulence via a simplified algebraic model for fill levels which extend above the height of the paddle impeller. Evidently, from the perspective of efficient production, it is advisable that the fill level is kept above this height when mixing to prevent pockets of stagnant fluid forming, which can prevent mixing for extended periods due to the segregation induced. Therefore, if small batches are produced (within this viscosity range) it would be inadvisable to use a large scale production vessel and assume that production time would be reduced due to the smaller volume being processed; suitable scaled production tanks or paddle impellers would be required. This work has also highlighted the need for SMEs to understand the mixing mechanisms at work within their production vessels, to allow for the most efficient production. It is proposed that the reported CFD model can be used to assess the effect of further operational parameters on efficient mixing, including but not limited to, the effect of paddle speed and the alteration of tank geometry.

8. Acknowledgements

The work described in this paper was carried out as part of the Advanced Sustainable Manufacturing Technologies (ASTUTE) project (ref. numb. 80380). ASTUTE has been part-funded by the European Regional Development Fund through the Welsh Government, and the authors would like to acknowledge this funding. The authors would like to personally thank Cultech Ltd. and specifically Dr Sue Plummer, for the information provided on the application of stirred vessel mixing in large scale batch production.

References

[1] AIChE Equipment Testing Procedure in Mixing Equipment (Impeller Type) 3rd Edition. AIChE, New York (2001)
[2] Guhu, D., Dudukovic, M.P., Ramachandran, A., Mehta, S., Alvare, J.: CFD-based compartmental modeling of single phase stirred-tank reactors. J AIChE. 52, 1836-1846 (2006)
[3] Dalian University of Technology, Chapter 6: Mixing, http://ceb.dlut.edu.cn/uploads/soft/110415/7-110415154330.pdf (retrieved March 2012), (2010).

[4] Holland, F.A., Chapman, F.S.: Liquid Mixing and Processing in Stirred Tanks. Chapman and Hall Ltd., (1966)
[5] Ein-Mozaffari, F., Upreti, S.R.: Investigation of Mixing in Shear Thinning Fluids using Computational Fluid Dynamics. Ryerson University, Toronto (2010)
[6] Nere, N.K., Patwardhan, A.W., Joshi, J.B.: Liquid-phase mixing in stirred vessels: Turbulent flow regime. Ind. Eng. Chem. Res. 42, 2661-2698 (2003)
[7] Rahimi, M., Parvareh, A.: Experimental and CFD investigation on mixing by a jet in a semi-industrial stirred tank. Chem. Eng. Jou. 115, 85-92 (2005)
[8] Kim, Y., Park, S.: Navier-Stokes simulation of unsteady rotor-airframe interaction with momentum source method. Int. J. of Aero. & space sciences. 10, 125-133 (2009)
[9] Brucato, A., Ciofalo, M., Grisafi, F., Micale, G.: Numerical prediction of flow fields in baffled stirred vessels: A comparison of alternative modeling approaches. Chem. Eng. Sci. 53, 3653-3684 (1998)
[10] Smith, F.G.: A model of transient mixing in a stirred tank. Chem. Eng. Sci. 52, 1459-1478 (1997)
[11] Choi, B.S., Wan, B., Philyaw, S., Dhanasekharan, K., Ring, T.A.: Residence Time Distributions in a Stirred Tank: Comparison of CFD Predictions with Experiment. Ind. Eng. Chem. Res. 43. 6548-6556 (2004)
[12] Montante, G., Mostek, M., Jahoda, M. Magelli, F.: CFD simulations and experimental validation of homogenization curves and mixing time in stirred Newtonian and pseudoplastic liquids. Chem. Eng. Sci. 60. 2427-2437 (2005)
[13] Buwa, V., Dewan, A., Nassar, A.F., Dunst, N.F.: Fluid dynamics and mixing of single-phase flow in a stirred vessel with a grid disc impeller: Experimental and numerical investigations. Chem Eng. Sci. 61. 2815-2822 (2006)
[14] ANSYS Inc.: ANSYS FLUENT User's Guide Release 14.0. ANSYS Inc., Canonsburg, PA (2011)
[15] Launder, B.E., Spalding, D.B.: The numerical computation of turbulent flows. Comp. Methods in App. Mech. & Eng. 3. 269-289 (1974)
[16] Croft, T.N., McBride, D., Cross, M., Gebhardt, J.E.: Multi-component free surface flows and rotating devices in the context of minerals processing. Int. J. of Comp. Fl. Dy. 23 93-107 (2009)
[17] Montante, G., Magelli, F.: Liquid Homogenization Characteristics in Vessels Stirred with Multiple Rushton Turbines Mounted at Different Spacings: CFD Study and Comparison with Experimental Data. Chem. Eng. Res. & Des. 82. 1179-1187.
[18] ANSYS Inc.: ANSYS ICEM CFD User's Manual Release 14.0. ANSYS Inc., Canonsburg, PA (2011)